Surface Science 604 (2010) 1784–1790

Contents lists available at ScienceDirect

Surface Science

journal homepage: www.elsevier.com/ locate/susc

Stability of siloxane couplers on pure and fluorine doped SnO_2 (110) surface: A first principles study

V. Golovanov [a,b,*], M. Viitala [a], T. Kortelainen [a], O. Cramariuc [a], T.T. Rantala [a]

[a] Department of Physics, Tampere University of Technology, P.O. Box 692, FI-33101 Tampere, Finland
[b] South-Ukrainian University, Staroportofrankovskaya Str., 26, 65008, Odessa, Ukraine

ARTICLE INFO

Article history:
Received 3 May 2010
Accepted 5 July 2010
Available online 15 July 2010

Keywords:
Density functional calculations
Stannic oxide
Siloxane coupler
Grafting

ABSTRACT

Siloxane is a favorable candidate as an anchor group that can be used to bind organic molecules to SnO_2 surfaces, with a wide range of practical applications. Therefore, adsorption geometries and energies of siloxane coupler on the SnO_2 (110) surface have been investigated in this study using quantum-chemical periodic density functional theory (DFT) calculations. We present a comparative study of different siloxane adsorption arrangements on pristine and fluorine doped SnO_2 surface. According to the calculations, the surface doping with fluorine leads to stabilization of the siloxane network at the stannic oxide surface. The trend is analyzed in terms of additional charge provided by F impurities to the chemisorbed oxygen atoms thus increasing the ionicity of their bonding. Implications of the current findings for the design of organic-metal oxide interface with better thermo-stability and improved electronic properties are discussed.

1. Introduction

Stannic oxide (SnO_2) is widely used as gas sensing material showing high sensitivity, fast response and short recovery times. Although, both bare and noble metal doped SnO_2 have extensively been studied in the past [1], functionalizing of oxide surfaces with organic or even bioactive components offer a new avenue for expanding their sensing properties. Due to the variety of chemical and structural modifications offered by organic materials the composite sensors can be expected to exhibit specific response to a particular gas or bio molecules [2]. Therefore, large opportunities appear for applications in chemical sensing and catalysis [3,4], biology and biomedicine [5,6]. For surface modification purposes one of the best-known coupling agents is based on siloxane derivatives [7] that can be used to bind a wide range of molecules to the SnO_2 surfaces. By a subsequent modification of the layers that contain reactive end-functional groups, a number of functionalized organic surfaces can be prepared [8].

Further progress in applications of such structures would still be possible if some remaining fundamental problems of hybrids, such as their medium to low stability and sensitivity could be overcome. The operating temperature of the hybrid is usually restricted by sustainability of the organic component. Besides, the monolayer or even thicker siloxane network may sterically hinder the charge transfer across the organic–inorganic interface. Both of these factors may slow down the rate of chemical reactions at the surface resulting in lower sensitivity to the target analyte. In the work of I. Matsubara et al. [9], an increased selectivity to carbon monoxide was achieved by functionalizing the SnO_2 films with amine groups anchored via organosilane coupling molecules. However, the sensitivity threshold of the constructed sensor was limited to 3% of CO at maximum allowable operating temperature of 125 °C.

In order to enhance the electrochemical communication through organically grafted metal oxide surfaces, the linker groups responsible for the molecular receptors formation need to be able to transport electronic charge across their molecular backbones. First principles modeling provides invaluable information on the type of bonding, the charge transfer reaction pathway and the activation barriers for the charge transfer across the organic–inorganic interface.

Stability of the siloxane spacer at the metal oxide surface may be limited by the low-temperature decomposition of the surface oxygen atoms. Thus, optimum conditions to the layer self-assembling must be aimed at further reinforcement of the generated entity either by post-treatment of the layer (e.g., formation of hydrogen and other dipolar bridges) or by pre-treatment procedures, which include formation of a certain type of oxygen vacancies or specific doping with “surface anchors”. These elements can be readily chosen on the basis of *ab initio*-DFT calculations.

The promising case to be tested theoretically is the fluorine doped tin oxide films. Fluorine is inexpensive, and therefore, these films are widely used as transparent and conductive sensing electrodes in organic photovoltaic devices [10–12] or electrochemically active coatings [13]. The presence of the SnO_2:F underlayer may bring a new functionality to the photo-electro-chemically active layers self-assembled on the surface of tin oxide films using the siloxane chemistry [14].

* Corresponding author. Department of Physics, Tampere University of Technology, P.O. Box 692, FI-33101 Tampere, Finland.
E-mail address: alban@te.net.ua (V. Golovanov).

0039-6028/$ – see front matter © 2010 Elsevier B.V. All rights reserved.
doi:10.1016/j.susc.2010.07.006

In a faceted SnO_2 sample, the lowest indices (110) stoichiometric surface is the most likely to be favored from the thermodynamic point of view. Therefore, and motivated by the importance of siloxane spacer to the function of any SnO_2 based hybrid device, we generate models of the siloxane layer grafted to pure and fluorine doped SnO_2 (110) surfaces and predict their relative stability and functionality using DFT calculations.

2. Computational methods and models

All our calculations are based on the Density Functional Theory (DFT) and exchange-correlation is included within the generalized gradient approximation (GGA) with parameterization by Perdew, Burke and Ernzerhof (PBE) [15]. The GGA electron densities are known to be good enough for the chemical insight, and most importantly, the cancellation of errors improves the accuracy in comparison of different geometries and large energy differences, which is the case in our study.

Periodicity and linear combination of atomic orbitals (LCAO) approach are applied. The advantages in employing LCAO (compared to the plane-wave (PW) basis) are the relatively small basis set and unlimited choice of vacuum thickness in between slabs. Also, the LCAO gives a comprehensible description of the molecule–surface interaction in terms of molecular orbitals and substrate bands. Additionally, the LCAO basis also gives the possibility to directly project atomic charges onto atomic or molecular orbitals which gives good chemical intuition when considering bonding [16]. Where relevant, the charge distribution analysis is also performed with Hirshfeld Method [17] that gives basis set independent information about the atomic contributions. Our calculations have been performed using the Dmol3 software [18].

The basis functions are one-electron orbitals of free atoms and ions computed in a numerical form prior to the crystal calculations. The spatial basis cut-off is 4.9 Å. All electron basis sets are used for all the elements. The specific basis set used in the calculations is sc. "double numerical basis with polarization functions" (DNP) [18]. It contains a polarization d function on heavy atoms and a polarization p function on hydrogen. It is comparable in size with the 6-31G** Gaussian basis set. However, numerical basis sets of a given size are considered to be more accurate than Gaussian basis sets of the same size.

For modeling the surfaces we use the standard procedure by first finding the relaxed bulk geometry. The bulk lattice constants of $a = 4.82$ Å, $c = 3.29$ Å obtained by total energy minimization with a $5\times5\times8$ Monkhorst–Pack k-point sampling agree well with the experimental values of $a = 4.74$ Å, $c = 3.19$ Å. GGA band gap is underestimated by about 2.0 eV as compared to the experimental value of 3.6 eV. This is expected, as GGA tends to overestimate the lattice constant and underestimate the band gap. "Thermal smearing" of 0.136 eV was used to speed convergence but due to the large band gap the effect on the occupation of bands is negligible.

Next, the SnO_2 (110) surfaces are built by cleaving from the above bulk crystal and placing a vacuum space of 40 Å between slabs to ensure sufficient separation between periodic images in the vertical direction. The same computational parameters as in the bulk calculation are employed for the slab model except for the k-point sampling $2\times4\times1$, which is consistent with the bulk calculation with the smaller super cell. For finding the consistently relaxed surfaces with and without adsorbates we follow the standard procedure. The center layer atoms are fixed to bulk geometry during the relaxation of the slab while allowing all the other atoms of the substrate and adsorbed molecules to relax. This results in the sc. equilibrium geometry. Fig. 1 illustrates the tin dioxide crystal and its (110) surface.

A slab model with five $O(Sn_2O_2)O$ atomic layers including 150 atoms in the supercell (5×1, 16.5×6.8 Å)) was used for modeling of the stoichiometric SnO_2 (110) surface. Several possible scenarios were selected as starting configurations for the relaxation of the SnO_2–siloxane systems. We have considered silicon in 4-fold coordination, wherein Si binds to the surface via three O atoms, located in bridging (O_{br}), in-plane ($O_{in\text{-}pl}$) and on-top of 5-fold tin atom (O_{Sn5f}) positions, see Fig. 1. The reactive functional group (R) in the Si–R bond was modeled with a single hydrogen atom at this first stage. In the molecular adsorption studies, the geometry of the siloxane spacer was first relaxed when placed on different sites at the SnO_2 surface. The coverage was 0.2 (the coverage is defined as the ratio between the number of adsorbed siloxane molecules and the number of surface 5-fold Sn atoms). These optimized geometries were studied then by comparative evaluation of their energetics, partial and total densities of states (DOS), Hirshfeld charges, and bond populations.

The definition of stability for Si-linker is however ambiguous as its interaction with surface can be determined in several ways. In most arrangements, silicon is coordinated by one or two chemisorbed O_{Sn5f} (in doped cases F atoms), which can be included in adsorbate complex or treated separately. In the first approach, adsorption (or interaction) energies have been calculated by computing the difference in minimized energies between the clean SnO_2 surface (E_{slab}) plus whole siloxane complex, involving O_{Sn5f} atoms (and in some doped cases F atoms) in the gas phase (E_{silox}) and the total energy of the combined system of substrate and adsorbate ($E_{silox@slab}$), i.e. $E_{ads}^{silox} = (E_{slab} + E_{silox}) - E_{silox@slab}$. A positive value thus indicates stable adsorption. The shortcoming of this method arises from necessity to compare the adsorption energies of different complexes on pristine SnO_2 surface. One of the possible alternative approaches may consist

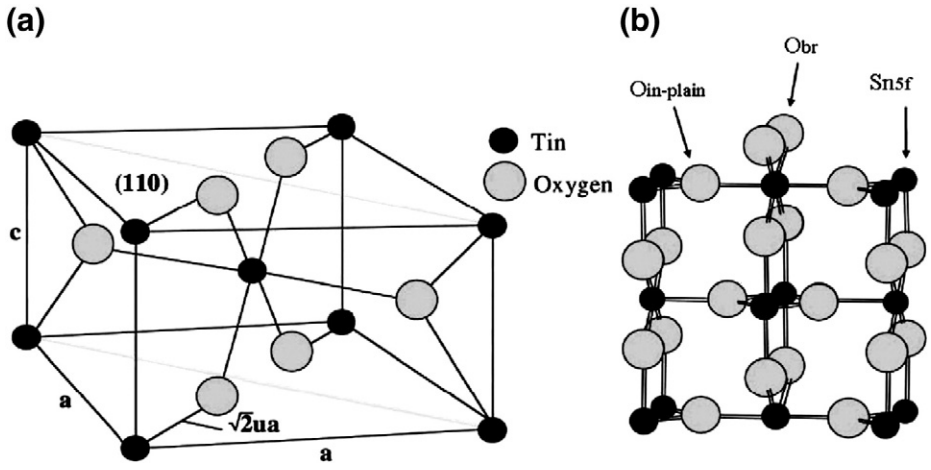

Fig. 1. (a) Tin dioxide crystal unit cell and its (110) surface. (b) Slab 1×1 supercell with two layers of (110) surface with the top face stoichiometric and the bottom face reduced. Tin atoms in the corners of the supercell are 5-fold (Sn_{5f}), the centermost surface oxygen atoms are 2-fold (bridging oxygen (O_{br})) and in-plane surface oxygen atoms are 3-fold ($O_{in\text{-}pl}$).

in calculation of the adsorption energies of the very same adsorbate, namely interaction of SiH group (key linker to organic molecules) with the whole oxygen/fluorine subsystem of SnO_2 surface. Thus, $E_{ads}^{SiH} = (nE_{O/F@slab} + E_{SiH}) - E_{silox@slab}$, where E_{SiH} is the total energy of the SiH molecule in gas phase and $nE_{O/F@slab}$ is the minimized total energy of the slab with n oxygen or fluorine atoms chemisorbed on-top of corresponding 5-fold tin atom. It is worth noting that in our estimations E_{ads}^{SiH} appeared to be much higher than E_{ads}^{silox}. Therefore, for description of the stability of siloxane coupler we further consider only relevant E_{ads}^{silox} data.

Our model neglects effects from the finite temperature and ambient atmosphere, which control the oxygen contents of SnO_2 surfaces. Therefore, we have also considered the effect from oxygen atmosphere on the relative stabilities of the compared adsorbate/surface structures. Reasonable temperatures or changes in oxygen pressure (chemical activity) are not found to have essential effect on the relative energetics and are far from changing the order of stabilities. Therefore, these issues are not explicitly included in the energetics, below, but only the zero-Kelvin adsorption energies are given, as defined above.

3. Results and discussion

3.1. SnO_2(110)–siloxane system

Series of coupling configurations were generated by placing SiH group around the points of high symmetry with respect to the double-sided stoichiometric slab and relaxing the whole structure, see Fig. 2.

Table 1
Inter-ionic distances (Å) and adsorption energies (eV) for the various scenarios from Fig. 2(a–d).

Adsorbate	Sn_{5f1}–O_{Sn5f1}	Sn_{5f2}–O_{Sn5f2}	Si–O_{Sn5f1}	Si–O_{Sn5f2}	Si–O_{br}	E_{ads}^{silox}
a) SiH	–	–	–	–	1.58	4.3
b) SiHO	2.07	–	1.64	–	1.69/1.72*	5.8
c) SiHOO	2.06	2.17	1.64	1.69	1.75	4.0
d) SiHOO + Vo_{in-pl}	2.20	2.08	1.82	1.61	1.68	5.3

*The distances to both adjacent O_{br} are presented.

The computed data for each of the adsorption modes are presented in Table 1 (local geometries and adsorption energies) and Table 2 (population analysis).

Strong relaxation of the adsorbed complexes was observed when in-plane oxygen atoms were initially involved in bonding of the siloxane spacer to the SnO_2 (110) surface. Thus, optimization of the geometry, where three-fold Si was coordinated via one in-plane and two bridging oxygen atoms results in relatively less stable bidentate structure (Fig. 2a). Testing of several surface geometries permits us to conclude that neither in-plane oxygen nor 5-fold Sn surface atoms (Sn_{5f}) are the chemically active sites for bonding of siloxane network at tin oxide (110) surface. It is worth noting that formation of the bridging oxygen vacancy reveals the 5-fold tin atoms, which according to our estimations are not a favorable surface site for adsorption of Si-linker. Therefore, we further focus on the several geometries that involve both O_{Sn5f} and O_{br} atoms, which are abundant on the surface in oxygen rich conditions.

The most stable configuration of the siloxane complex is formed when silicon is coordinated via two O_{br} and one O_{Sn5f} atoms (Fig. 2b).

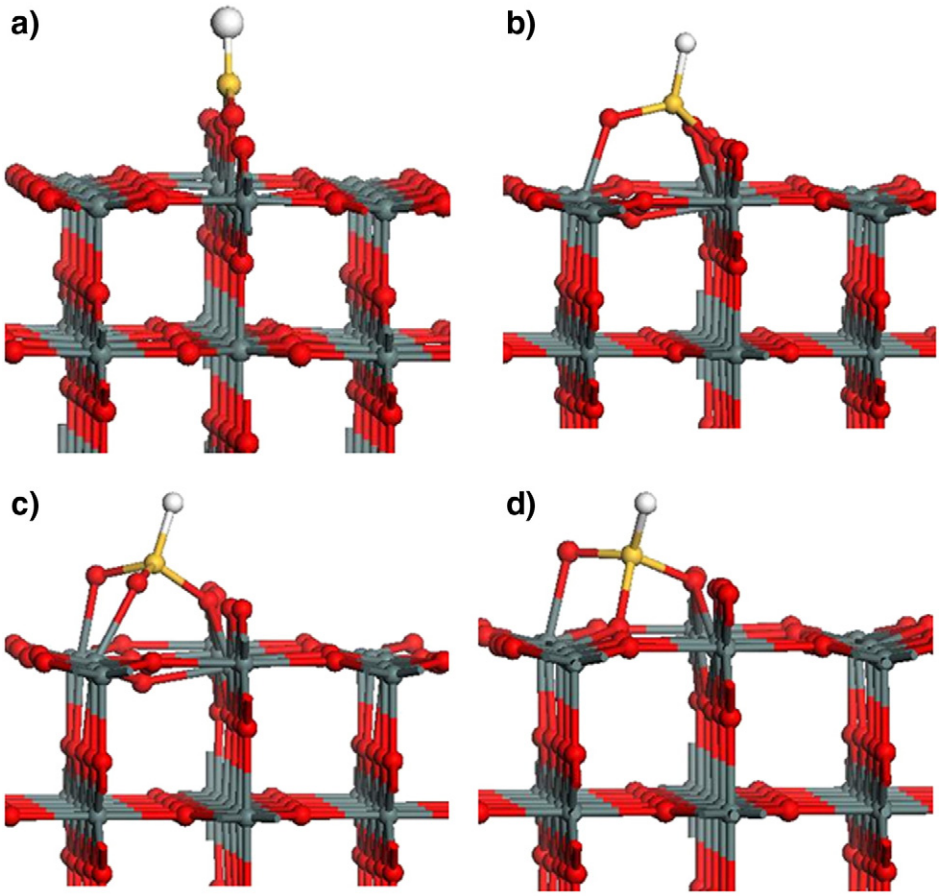

Fig. 2. Optimized structures of siloxane spacer at SnO_2 (110) surface coordinated via: a) two O_{br} and one O_{in-pl} atoms; b) two Obr and one O_{Sn5f} atoms and c) two O_{Sn5f} and one O_{br} atoms. d) The relaxed geometry from figure c) with in-plane oxygen vacancy formed below the Si atom. The gray spheres represent tin atoms and the red ones oxygen atoms. Silicon and hydrogen are depicted in yellow and white.

Table 2
Hirshfeld population-derived charges (|e|) for the various scenarios from Fig. 2(a–d).

Adsorbate	O_{Sn5f_1}	O_{Sn5f_2}	Sn_{5f_1}	Sn_{5f_2}	Si	O_{br}
a) SiH	–	–	–	–	+0.54	−0.31/−0.33*
b) SiHO	−0.36	–	+0.70	–	+0.42	−0.38/−0.33*
c) SiHOO	−0.32	−0.28	+0.68	+0.73	+0.42	−0.32
d) SiHOO + Vo_{in-pl}	−0.35	−0.28	+0.70	+0.75	+0.45	−0.31

*The charges of both adjacent O_{br} are presented.

On the contrast, arrangement with two chemisorbed O_{Sn5f} atoms results in the worst-possible interaction of the coupler with the SnO_2 surface (Fig. 2c). The significant difference in adsorption energies between the whole anchor group and SiH molecule (estimated by the second approach) for this conformation is connected with the fact that in the first case the O_{Sn5f}–Si interaction is not included in the calculation of adsorption energy. We can deduce therefore that the weakest interaction in Sn–O_{Sn5f}–Si bond occurs particularly between the Sn and O_{Sn5f} atoms. This conclusion correlates with the corresponding bond lengths, see Table 1.

The prominent feature in the most energetically favorable geometry (Fig. 2b) is a downward displacement (~0.5 A) of in-plane oxygen atom located below the siloxane complex. Such relaxation can be connected with additional charge accumulated (according to Hirshfeld population analysis) at surface Sn_{5f} atoms due to coupling with siloxane. Hence, attraction between the O_{in-pl} and the nearest cations decreases causing the downward relaxation of the in-plane oxygen atom. Tin Sn_{5f} cations gain the Hirshfeld charge from the oxygen atoms (O_{Sn5f}) chemisorbed on-top of them pointing out on the covalent nature of this bonding. These O_{Sn5f} atoms are featured by considerably reduced valence charge with respect to bulk O ions and therefore can be labeled as O^- ions. Removal of the in-plane oxygen atom and formation of the surface oxygen vacancy leads to stabilization of the whole system (Fig. 2d). In this case a strong relaxation is induced by one of the O_{Sn5f} atoms tending to occupy the in-plane oxygen vacancy site.

The deficiency of the negative charge in siloxane system, needed for establishing a strong ionic bonding between the chemisorbed oxygens and 5-fold tin atoms play a key role in the stabilization of the siloxane spacer at the SnO_2 surface. This charge can be injected from supporting surface at the temperature above 0 K through the thermal population of the hybridized energy states of O_{Sn5f} and Sn_{5f} atoms located around 0.5 eV above the VBM. These states were observed in the calculated DOS projected onto atomic orbitals of corresponding oxygen and tin atoms (not shown). Alternatively, the surface doping with fluorine that brings additional electrons to the system may have two-fold benefits: facilitating the charge transport through the spacer and improving of its stability.

3.2. Fluorine doped SnO_2 (110)–siloxane system

For low fluorine content F^- anion substitutes for an O^{2-} anion in the lattice (Fo) and oxygen vacancies sites, thus creating more free electrons [19]. Increase of doping concentration above the specific level results in F occupying interstitial positions (Fi), which is inactive as a single dopant, but act as a compensating acceptor in highly doped n-type SnO_2 where FoFi are formed [20,21]. This explains the measured non-linear dependence of the resistivity with respect to the F content [22–24]. The combined XRD and XPS study demonstrates that the concentration of the fluorine atoms inside the grains is several times lower than that in the grain boundaries [25]. Theoretical analysis based on DFT calculations of the rutile TiO_2 (110) structure reveals that besides substituting the oxygen sites, F^- ions may coordinate to surface Ti^{4+} ions [26].

Based on the examination of the experimental and theoretical works listed above, we therefore considered several scenarios for SiH group coordinated to the fluorine doped SnO_2 (110) surface, where O_{in-pl}, O_{Sn5f_1} and O_{Sn5f_2} oxygen atoms were sequentially substituted by the F anions, see Fig. 3. The optimized structural parameters, adsorption energies and Mulliken population-derived charges of these conformations are listed in Tables 3 and 4.

It was found that surface doping with fluorine makes the siloxane spacer considerably more stable, when F atom is substituting O_{in-pl} (Fig. 3b). The corresponding binding energy is increased approximately by 1.7 eV (comparing with the case depicted in the Fig. 3a). Fluorine ions adsorbed on-top of Sn_{5f} reduces the coupler's binding energy. However, the replacing of atom O_{Sn5f_2} with F leads to a breaking of the Sn_{5f}–F bond and formation of tetrahalide-like structure, which is still energetically favorable.

In their paper Xu et al. [27] dealing with DFT calculations of the bulk doped SnO_2:F structure do not observe any significant change in the charge density distribution by introducing the F impurity. In our study, however, the essential redistribution of the charge density caused by replacing of O atoms by F is detected. This disagreement may be connected with surface location of the F dopants in our case. The presence of the F 2p states in the conduction band reported in [27] for bulk substituted Fo system is consistent with the donor behavior of F defect at moderate doping level (0.5 to 3 at.%) [22–24,28]. For the geometries depicted in Fig. 3(b–d), we do not detect noticeable coupling between the conduction band and the levels localized at the fluorine site. Instead, the resonance with siloxane system became evident in the corresponding DOS peaks. We suggest therefore that the excess electron of F impurity (while located at surface) affects the charge density distribution in the siloxane system rather than being injected into the conduction band at non-zero temperatures.

The Hirshfeld charge of F-on-O_{in-pl} (Fig. 3b) averages to only half of the valence charge of the bulk O atoms. Since the latter ones are commonly designated as O^{2-} ions, the fluorine atom occupying the in-plane oxygen position can be attributed to F^- ion. In this geometry both O_{5f} atoms gain substantial negative charge (~10% for O_{5f_1} and ~20% for O_{5f_2}), which became now comparable with the valence charge of the bulk oxygen atoms. We conclude therefore that the O^- ions chemisorbed on-top of Sn_{5f} atoms upon introducing fluorine dopant transforms to O^{2-} thus increasing the ionicity of the Sn_{5f}–O_{5f} bonds. This is consistent with the significant loss of negative charge by the corresponding Sn_{5f} atoms as well as with decrease of the Sn_{5f}–O_{5f} bond length (e.g. from 2.17 Å to 2.043 Å for O_{5f_2} atom).

The binding energy of Sn–F bond is lower than that of Sn–O bond (4.85 eV and 5.48 eV, respectively). This can explain significantly more pronounced downward relaxation of Fo_{in-pl} (1.2 Å) as compared with its substituted counterpart (Fig. 3b). The lower electrostatic interaction with F^- ion is also a reason of considerable elongation (on average 8%) of the Sn_{5f}–Fo–Si bond (Fig. 3c), which was finally split in configuration depicted in Fig. 3d.

The charge redistribution in scenarios presented in Fig. 3c–d only marginally differs from the case above. The essential change in both these geometries is a conversion of the remaining chemisorbed O^- anion to O^{2-}. The amount of charge gained by the O_{5f} atoms is in clear correlation with its evaluated adsorption energy, i.e. the larger charge increment at O_{5f} ion the more firmly it is bound to SnO_2 surface. Thus, F impurity adsorbed on-top of 5-fold Sn atoms has dual effect on stability of the organosilane spacer. On the one hand, E_{ads}^{silox} is decreasing due to a weak Sn–F bond. Even minor elongation provokes its easy splitting (Fig. 3d). On the other hand, corresponding charge redistribution reinforces the remaining Sn–O binding that makes resulted bidentate structure energetically favorable.

The corresponding transformations that occur in the calculated DOS of pure and fluorine doped SnO_2 grafted with siloxane are presented in Fig. 4. The new peaks appeared near the VBM of SnO_2 slab due to adsorption of siloxane complex (Fig. 4a). They are associated with O_{5f} and O_{br} atoms involved in bonding. The low-lying

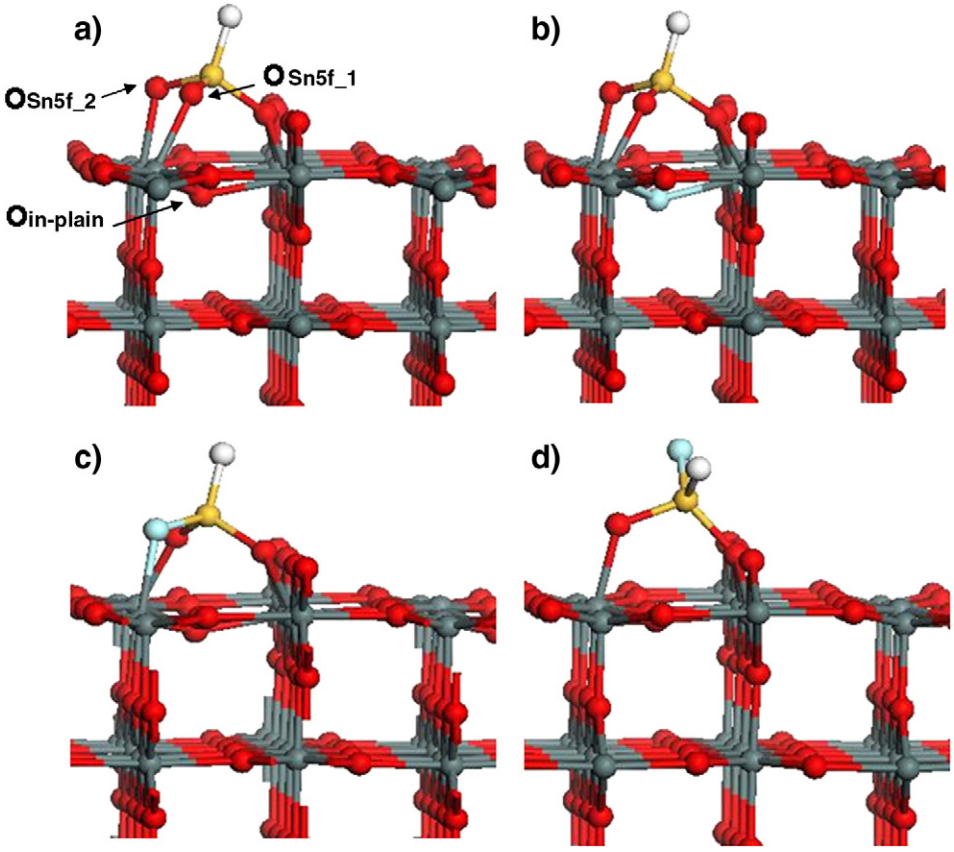

Fig. 3. Optimized structures of siloxane spacer at pure (a) and fluorine doped (b–d) SnO_2 (110) surface. In the case (b) the $O_{in\text{-}pl}$ was substituted by F atom. In the cases (c) and (d) O_{Sn5f_1} and O_{Sn5f_2} were respectively substituted by the F atom. The gray spheres represent tin atoms and the red ones oxygen atoms. Silicon, hydrogen and fluorine depicted in yellow, white and blue.

3d-type of orbitals of the silicon covalently hybridize with p-orbitals of oxygen atoms in a distorted trigonal bipyramid.

The most visible modification in DOS of the F-on-$O_{in\text{-}plain}$ system is the shift to higher energies of the peaks associated with chemisorbed oxygen atoms (Fig. 4b), which is consistent with increased ionicity of their bindings. Indeed, the changes observable in PDOS of O_{Sn5f_2} atom from the configuration depicted in Fig. 3b (not shown here for the sake of brevity) include the shift of the peak at 0.46 eV to higher energies (~0.7 eV). The notable contribution of s-orbitals to this peak points out that these states are characteristic of Sn–O bond. The similar shift (0.46 eV→1.17 eV) was found in PDOS of corresponding Sn_{5f} atom. These changes are accompanied by the shortening of Sn–O distance. Along with loss of negative charge by the corresponding Sn atom (making it Sn^{4+}) and increase of the negative charge at the O ion (making it equal to O^{2-}) it may indicate that ionicity of the Sn–O binding is increased. In PDOS of Si the corresponding shift (0.46 eV → 1.17 eV) is clearly seen indicating that the whole Sn–O–Si bond is affected. All above mentioned transformations, but less pronounced occur for O_{Sn5f_1} atom (e.g., new peak appears at 1.17 eV). The less expressed changes may be connected with the fact that O_{Sn5f_1} atom has initially higher amount of the negative valence charge. The similar trends were observed for cases (c) and (d).

From PDOS analysis we found that hybrid low-energy peak attributed to the covalent Sn_{5f}–O_{5f} bonding decrease in proportion to amount of charge received by the chemisorbed oxygens upon doping. Concurrently, the electron density of the oxygen atoms populates the 3d atomic orbitals of the O–Si bond that is evident in the total DOS from the shift and increase of the peak at 0.1 eV to lower energies. The basic changes observed in the DOS of F-on-O_{5f} systems (Fig. 4c–d) are in the course of our previous findings.

Table 3
Inter-ionic distances (Å) and adsorption energies (eV) for the various scenarios from Fig. 3(a–d).

Adsorbate	Sn_{5f1}–O_{Sn5f1}	Sn_{5f2}–O_{Sn5f2}	Si–O_{Sn5f1}	Si–O_{Sn5f2}	Si–O_{br}	E_{ads}^{silox}
a) SiHOO	2.06	2.17	1.64	1.69	1.75	4.0
b) SiHOO + $Fo_{in\text{-}pl}$	2.02	2.04	1.64	1.66	1.75	5.7
c) $SiHOFo_{Sn5f\_1}$	2.25*	2.10	1.75*	1.63	1.68	3.1
d) $SiHOFo_{Sn5f\_2}$	2.04	–	1.63	1.61*	1.71	4.3

*The corresponding O atom is replaced with F.

4. Conclusion

Adsorption of organic molecules on the SnO_2 surfaces is widely used in a number of technological applications, where in most cases the organic molecules are grafted to the SnO_2 (110) surface through a siloxane group. A key step is the understanding of the nature of the silicon–oxygen–stannic bonds on such surface, which was the specific objective of our *ab initio* study. By using DFT computational methods, we have studied the siloxane coupler on the stoichiometic SnO_2 (110) surface and the effect of fluorine doping on its stability. It

Table 4
Hirshfeld population-derived charges (|e|) for the various scenarios from Fig. 3(a–d).

Adsorbate	O_{Sn5f_1}	O_{Sn5f_2}	Sn_{5f_1}	Sn_{5f_2}	F	Si	O_{br}
a) SiHOO	−0.32	−0.28	+0.68	+0.73	–	+0.42	−0.32
b) SiHOO + $Fo_{in\text{-}pl}$	−0.34	−0.33	+0.70	+0.75	−0.18	+0.42	−0.32
c) $SiHOFo_{Sn5f\_1}$	–	−0.34	+0.71	+0.74	−0.14	+0.45	−0.34
d) $SiHOFo_{Sn5f\_2}$	−0.36	–	+0.71	+0.80	−0.18	+0.45	−0.31

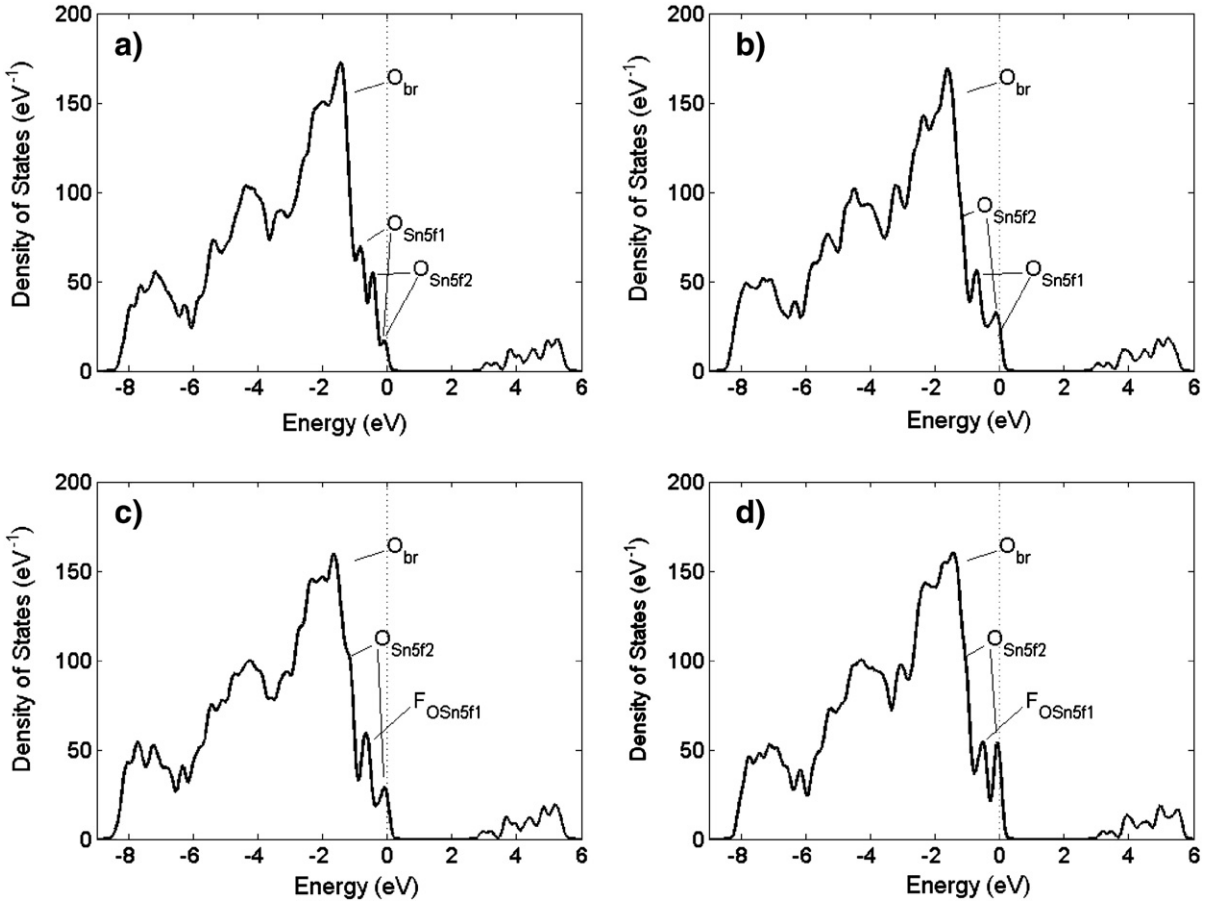

Fig. 4. Density of states (DOS) of the SnO_2 (110) surface. The stoichiometric surface with siloxane complex is shown in the panel a). In the case (b) the $O_{in\text{-}pl}$ was substituted by F atom. In the cases (c) and (d) O_{Sn5f_1} and O_{Sn5f_2} were respectively substituted by the F atom.

was found that neither in-plane oxygen nor 5-fold Sn surface atoms are the chemically active sites for bonding of Si-linker at stannic oxide (110) surface. The most favorable configurations include silicon coordinated at the tin oxide surface via one chemisorbed and two bridging oxygen atoms. The weakest point of the siloxane coupler with respect to its stability is the bond between the chemisorbed oxygen and the five-fold tin atom. It is indicative that this particularly bond is mainly affected by the introducing of fluorine. Removal of the in-plane oxygen atom and formation of the surface oxygen vacancy leads to stabilization of the whole system. Thus, an appropriate surface pattering may be a useful technological step in grafting procedure.

Our calculations show that the dominant role of F impurities at the surface in providing of additional charge to the siloxane system. This is accompanied by transformation of the O^- ions chemisorbed on-top of Sn_{5f} atoms into O^{2-} thus strengthening the Sn–O–Si bonds. Therefore, we expect the stabilization of organosilane spacer at the fluorine doped SnO_2 (110) surface to result in improvement of the sensitivity of hybrid sensors. This is because the operating temperature can be substantially increased without detriment to sustainability of the grafted component.

References

[1] V.E. Henrich, P.A. Cox (Eds.), The Surface Science of Metal Oxides, Cambridge University Press, Cambridge, USA, 1994, 464 pp.;
T.T. Rantala, T.S. Rantala, V. Lantto, Materials Science in Semiconductor Processing 3 (2000) 103–107;
M.A. Mäki-Jaskari, T.T. Rantala, Surface Science 537 (2003) 168–178;
M.A. Mäki-Jaskari, T.T. Rantala, V.V. Golovanov, Surface Science 577 (2005) 127–138.
[2] Y. Ozaki, S. Suzuki, M. Matsunaga, Enhanced long-term stability of SnO_2-based CO gas sensors modified by sulfuric acid treatment, Sensors and Actuators B 62 (2000) 220–225.
[3] Lina Geng, et al., Characterization and gas sensitivity study of polyaniline/SnO_2 hybrid material prepared by hydrothermal route, Sensors and Actuators B 120 (2007) 568–572.
[4] W. Cardoso, M. Francisco, R. Landers, Co (II) porphyrin adsorbed on SiO_2/SnO_2/phosphate prepared by the sol–gel method, Application in electroreduction of dioxygen, Electrochimica Acta 50 (2005) 4378–4384.
[5] C. You, T. Miyazaki, E. Ishida, Bioactive organic–inorganic hybrids prepared from poly(vinylalcohol) via modification with metal oxides, Key Engineering Materials 309–311 (2006) 1153–1156.
[6] N. Jia, Q. Zhou, L. Liu, Direct electrochemistry and electrocatalysis of horseradish peroxidase immobilized in sol–gel-derived tin oxide/gelatin composite films, Journal of Electroanalytical Chemistry 580 (2005) 213–221.
[7] A. Fadeev, R. Helmy, S. Marcinko, Self-assembled monolayers of organosilicon hydrides supported on titanium, zirconium, and hafnium dioxides, Langmuir 18 (2002) 7521–7529.
[8] S. Toma, J. Bonacin, H. Toma Selective, Host–guest interactions on mesoporous TiO_2 films modified with carboxymethyl-b-cyclodextrin, Surface Science 600 (2006) 4591–4597.
[9] Ichiro Matsubara, Kouta Hosono, Norimitsu Murayama, Woosuck Shin, Noriya Izu, Organically hybridized SnO_2 gas sensors, Sensors and Actuators B 108 (2005) 143–147.
[10] R. Valski, C.D. Canestraro, L. Micaroni, R. Mello, L. Roman, Organic photovoltaic devices based on polythiophene films electrodeposited on FTO substrates, Solar Energy Materials and Solar Cells 91 (2007) 684.
[11] F. Yang, S.R. Forrest, Organic solar cells using transparent SnO2–F anodes, Advanced Materials 18 (2006) 2018–2022.
[12] E. Elangovan, K. Ramamurthi, Optoelectronic properties of spray deposited SnO_2: F films for window materials in solar cells, Journal of Optoelectronics and Advanced Materials 5 (1) (2003) 45–54.
[13] B. Correa-Lozano, Ch. Comninellis, A. de Battisti, Service life of Ti/$SnO_2 \pm Sb_2O_5$ anodes, Journal of Applied Electrochemistry 27 (1997) 970–974.
[14] V. Chukharev, T. Vuorinen, A. Efimov, N. Tkachenko, et al., Photo-induced electron transfer in self-assembled monolayers of porphyrin-fullerene dyads on ITO, Langmuir 21 (2005) 6385–6391.
[15] J.P. Perdew, K. Burke, M. Ernzerhof, Generalized gradient approximation made simple, Physical Review Letters 77 (1996) 3865–3868.

[16] R.A. Evarestov, Quantum chemistry of solids: the LCAO first principles treatment of crystals, first ed., Springer Series in Solid-State Sciences, 2007, p. 557.
[17] F.L. Hirshfeld, Bonded-atom fragments for describing molecular charge densities, Theoretica Chimica Acta B 44 (1977) 129–138.
[18] Anon., DMOL3 User Guide, Accelrys Inc., San Diego, 2007.
[19] S. Shanthi, C. Subramanian, P. Ramasamy, Preparation and properties of sprayed undoped and fluorine doped tin oxide films, Materials Science and Engineering B57 (1999) 127–134.
[20] C. Canestraro, M. Oliveirac, R. Valaski, M. da Silva, D. David, I. Pepe, A. Silva, L. Roman, C. Persson, Strong inter-conduction-band absorption in heavily fluorine doped tin oxide, Applied Surface Science 252 (2006) 5361.
[21] C. Canestraro, L. Roman, C. Persson, Polarization dependence of the optical response in SnO_2 and the effects from heavily F doping, Thin Solid Films 517 (23) (2009) 6301–6304.
[22] D.R. Acosta, W. Estrada, R. Castanedo, A. Maldonado, M.A. Valenzuela, Structural and surface studies of tin oxide films doped with fluorine, Thin Solid Films 375 (1998) 147–150.
[23] D.R. Acosta, E. Zironi, E. Montoya, W. Estrada, About the structural, optical and electrical properties of SnO_2 films produced by spray pyrolysis from solutions with low and high contents of fluorine, Thin Solid Films 288 (1996) 1–7.
[24] S. Aukkaravittayapun, C. Thanachayanont, T. Theapsiri, W. Veerasai, Y. Sawada, T. Kondo, S. Tokiwa, T. Nishide, Temperature programmed desorption of F-doped SnO_2 films deposited by inverted pyrosol technique, Journal of Thermal Analysis and Calorimetry 85 (3) (2006) 811–815.
[25] H. Cachet, A. Gamard, G. Campet, B. Jousseaume, T. Toupance, Tin dioxide thin films prepared from a new alkoxyfluorotin complex including a covalent Sn–F bond, Thin Solid Films 388 (2001) 41–49.
[26] A.M. Czoska, S. Livraghi, M. Chiesa, E. Giamello, S. Agnoli, G. Granozzi, E. Finazzi, C. Di Valentin, G. Pacchioni, The nature of defects in fluorine-doped TiO_2, Journal of Physical Chemistry C 112 (2008) 8951–8956.
[27] J. Xu, S. Huang, Z. Wang, First principle study on the electronic structure of fluorine-doped SnO_2, Solid State Communications 149 (2009) 527–531.
[28] B. Thangaraju, Structural and electrical studies on highly conducting spray deposited fluorine and antimony doped SnO_2 thin films from $SnCl_2$ precursor, Thin Solid Films 402 (2002) 71–78.